Exploring the Evolution of Post-acupuncture Resting-state Networks combining ICA and Multivariate Granger Causality

Chongguang Zhong, Lijun Bai, Ruwei Dai, Ting Xue, Yuanyuan Feng, Hu Wang, Zhenyu Liu, Youbo You and Jie Tian*, *Fellow, IEEE*

Abstract—The sustained effects of acupuncture have been widely applied to clinical treatment, thus it can be assumed that the relatively functional specificity of acupoints may evolve as the function of time. In this study, we originally combined ICA and multivariate Granger causality analysis to explore the causal interactions within and among the post-acupuncture resting-state networks (RSNs) at a hearing-related acupoint GB40, with the cognition-related acupoint KI3 as a control. Following acupuncture at GB40, the superior temporal gyrus (STG) and anterior insula (AI) within auditory network appeared persistent bidirectional connection with maximal strength, and the interactions between the auditory network and others became more complex as time passed. For KI3, both the superior parietal lobule (SPL) and dorsolateral prefrontal cortex (DLPFC), as vital nuclei of cognitive function, emerged increased causal outflows and inflows as time went on. We concluded that acupuncture at different acupoints may exert different evolutive effects on causal interactions within and across the RSNs during segmented post-stimulus resting states.

I. INTRODUCTION

ACUPUNCTURE, as an ancient therapeutic modality in Traditional Chinese Medicine, is widely applied to clinical treatment [1]. However, the neural mechanisms underlying the efficacy of acupuncture are not well established and need further exploration [2]. As one of modern in-vivo neuroimaging techniques, functional magnetic resonance imaging (fMRI) provides us an effective tool to map the effective connectivity of brain networks modulated by acupuncture.

Previous fMRI studies provide some evidence to support that acupuncture can modulate subcortical gray structures and the limbic-paralimbic-neocortical network in the human brain [3], [4]. These fMRI studies on acupuncture mainly focus on acute effects of acupuncture and spatial distributions of increased or decreased activities of brain regions during needling manipulations [5]. However, abundant clinical reports suggest that the analgesic effects of acupuncture may

Chongguang Zhong, Intelligent Medical Research Center, Institute of Automation, Chinese Academy of Sciences, Beijing, China. (e-mail: chongguang.zhong@ia.ac.cn).

Jie Tian, Intelligent Medical Research Center, Institute of Automation, Chinese Academy of Sciences, Beijng, China (Corresponding author, phone: 8610-82618465; fax: 8610-62527995; e-mail: tian@ieee.org)

last a long period even after the needling process being terminated [1]. Price et al. demonstrate that the analgesic effects of acupuncture may actually peak long beyond the needling session [6]. In this study, we focused on the sustained effects of acupuncture, rather than its acute effects.

Recent studies have already paid attention to the sustained effects of acupuncture [7], [8], and explored its impact on resting-state networks (RSNs) [9], [10]. Dhond et al. reveal that acupuncture can influence intrinsic connectivity in a resting brain network, i.e. default mode network (DMN) [9]. Another study also indicates that acupuncture may not only enhance the dichotomy of the anticorrelated resting-state networks, but also modulate the intrinsic coherences of the wide interoceptive-autonomic brain networks, including the paralimbic regions and brainstem nuclei [10]. Overall, acupuncture involves the interactions of multiple brain networks and acts in maintaining a homeostatic balance of the internal state within and across multiple brain systems. Although the studies mentioned above have explored the modulatory effects of acupuncture on multiple RSNs, little is known about the direction and strength of the information flow between multiple brain areas modulated by evolutive effects of acupuncture. In this study, we combined the independent component analysis (ICA) and multivariate Granger causality analysis (mGCA) to explore such evolutive causal interactions during segmented post-acupuncture resting states.

The data-driven method ICA can spatially isolate the spatial patterns of neuronal activity, such as function-related networks and artifacts (e.g. subtle movements, cardiac and respiratory pulsations) [11], [12]. The RSNs detected by ICA have also been proved to be highly reproducible and stable across subjects and sessions [11]. The bivariate Granger causality analysis may be an appropriate approach to explore the directional interactions within and among the RSNs detected by ICA, but it can't distinguish the direct or indirect causal connectivity [13]. The mGCA can overcome the deficiency by computing directed transfer function (DTF) from a multi-variate autoregressive model [14]. Therefore, mGCA has been employed to analyze causal relations among multiple brain areas simultaneously [14], [15]. To explore evolutive modulatory effects of acupuncture with combining ICA and mGCA would pave the way for a better understanding of neural mechanisms underlying acupuncture. We chose the acupoint KI3 as a control is used to obtain similar physiologic effects from a functional irrelevant

acupoint, because it is innervated by the same spinal nerve as GB40, albeit belonging to different meridians. We attempted to explore the relatively function specificity as time passed underlying acupuncture at different acupoints by comparing the effective connectivity patterns of the different segmented post-acupuncture resting states for the same acupoint, as well as different acupoints.

II. METHOD

A. Subjects

12 Chinese healthy right-handed volunteers (9 males, aged 23.5 ± 1.2) were recruited from a homogeneous group in this study. None of them had experienced neurological or psychiatric disorders. All subjects were acupuncture naïve and gave written informed consent as approved by the local ethics committee. All subjects were in accordance with the declaration of Helsinki.

B. Experimental Protocol

All subjects were instructed to close their eyes and remain relaxed, first underwent a 1 min "rest" scan with needle in GB40 (no needle manipulation), then three acupuncture manipulation epochs were separated by two intervals of 1 min "rest" period, finally a 6 min post-stimulus resting scan after removing the needle. To mitigate any potential long-lasting effects following the acupuncture intervention, another scan with the same experimental protocol at KI3 was performed 7 days later. A sterile disposable stainless steel acupuncture needle was applied to deliver acupuncture stimulation. The needle was rotated manually clockwise and counterclockwise for 1 min at 1Hz by a balanced "tonifying and reducing" technique [3]. The procedure was performed by the same experienced and licensed acupuncturist on all subjects. The precise locations of needling, the presumed acupuncture effects, and the stimulation paradigm were not divulged. Finally, the subjects were asked to quantify the throbbing, aching, soreness, heaviness, fullness, warmth, coolness, numbness, tingling, dull or sharp pain and any other sensations they experienced during the stimuli. The sensation rates from 0 to 10 (0 = no sensation, 1-3 = mild, 4-6 = moderate, 7-8 = strong, 9 = severe and 10 = unbearable sensation). The rate was used to distinguish deqi from pain. The subjects with obvious deqi or deqi was prominent than pain were chosen.

C. Image Acquisition and Preprocessing

Imaging data were acquired using a 1.5 Tesla ACS-NT15 Philips scanner. The images were parallel to the AC-PC line and covered the whole brain. Thirty axial slices were obtained using a T2*-weighted single-shot, gradient-recalled echo planar imaging sequence (FOV = 230 mm × 230 mm, matrix = 64 × 64, thickness = 5 mm, 0 mm gap, TR = 4000 ms, TE = 50 ms, flip angle = 90°). After the functional run, high-resolution structural information on each subject was also acquired using 3D MRI sequences with a voxel size of 1 × 1 × 1 mm³ for anatomical localization (TR = 2510 ms, TE = 15 ms, matrix = 384 × 512, FOV = 230 mm × 230 mm, flip angel = 30°, thickness = 5 mm).

All images during the post-stimulus resting period following acupuncture at GB40 and KI3 were pre-processed using statistical parametric mapping separately (SPM5, http://www.fil.ion.ucl.ac.uk/spm/). First, the image data underwent realignment for head motions using least-squares minimization. None of subjects had head movements exceeding 1 mm on any axis and head rotation greater than one degree. A mean image created from the realigned volumes was coregistered with the subject's individual structural T1-weighted volume image. Then, the standard MNI template provided by SPM5 was used in spatial normalization with resampling at 2 mm × 2 mm × 2 mm. These data were filtered by using a bandpass filter (0.01~0.08 Hz) to reduce the effect of low-frequency drift and high-frequency noise [16], [17]. Finally, all images were spatially smoothed with FWHM of 6 mm.

D. Data Analysis

A group spatial ICA was performed on fMRI data of all subjects during the 6 min post-acupuncture resting epochs using the GIFT software (http://icatb.sourceforge.net/). The images were reduced to 40 dimensions using principal component analysis, and the number of independent components (ICs) was estimated to be 25 using the MDL criteria [18]. Six ICs were identified by visual inspection as anatomically relevant areas across subjects based on the activation patterns [11], [12]. They included five coherent resting fluctuations functionally relevant regions involved in DMN, memory (included two ICs, bilateral brain), executive function, auditory processing and motor function (Fig. 1). The visual-related network was absent in this study because none of the stimulated acupoints was related to visual function. The maps of these ICs across all subjects were generated for a random effect analysis using a one-sample t-test (P < 0.05, correction using the false discovery rate (FDR) criterion). Then the values of t were converted to Z-values to indicate the voxels that contributed most strongly to a particular IC. In this study, voxels with absolute Z-values greater than 1.5 are considered as active for each IC.

Twelve regions of interest (ROIs) were selected in five functional brain networks [11]. They are the inferior temporal gyrus (ITG), anterior cingulate cortex (ACC) and posterior cingulate cortex/precuneus (PCC) within the DMN, the SPL, frontopolar area/prefrontal cortex (OFC) and middle temporal gyrus (MTG) within the memory network, the DLPFC and medial frontal gyrus (MeFG) within the executive network, the STG and AI within the auditory network, the postcentral gyrus and precentral gyrus within the motor network. The spherical ROIs were defined as the sets of voxels included in 6-mm spheres centered on the local maximum activation clusters extracted from ICA. For bilaterally activated regions, we only selected the hemisphere anatomical area with a more significant 'Z-score' as the

representative ROI. Then, the time series were averaged across voxels within each ROI. Finally, the averaged time course across subjects within each group was normalized to form a single vector per ROI.

The timeseries of BOLD signal intensities from these selected ROIs during the post-acupuncture resting state was divided equally into three phases (separately for each acupoint). Then we performed mGCA on fMRI data of each 2 min phase. The mGCA detected causal interactions between brain regions by computing DTF from a multivariate autoregressive model of the time series in the selected ROIs. The direct DTF (dDTF) was included in the mGCA process which could be interpreted in terms of Granger causality [19]. We also adopted the weighted DTF with partial coherence in order to emphasize direct connections and de-emphasize mediated influences. More details may be available on the study from Deshpande et al. [15]. To assess the significance of path weights, surrogate data were generated by randomizing the phase of the original time series spectrum while retaining its magnitude. A null distribution was obtained by generating 2500 sets of surrogate data and calculating the dDTF (for every connection) from these 2500 datasets [15], [19]. The dDTF value was compared with the null distribution for a one-tailed test of significance with a p-value of 0.05.
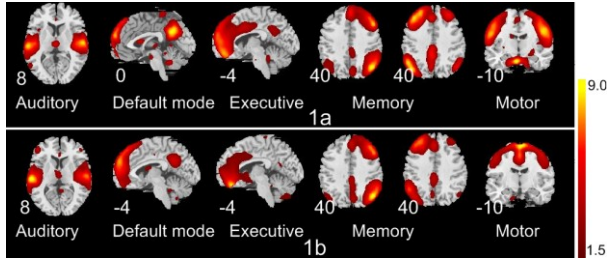

Fig. 1. Mean spatial independent components (brain activation networks) across subjects represented with a slice. Red to yellow is z values, ranging from 1.5 to 9.0. 1a denotes the five resting-state networks during post-stimulus at acupoint GB40, while 1b is for KI3.

III. RESULTS

The effective connectivity patterns of brain networks were described as directed graphs. The strength of causal connections was represented by the thickness of line which was divided into four grades with different colours (cyan-25%, yellow-50%, green-75%, red-100%), while the arrows indicated the direction of connections (Fig. 2). Only links that showed significant effective connectivity were presented in the maps (p < 0.05).

Figs. 2a, 2b and 2c refer to evolutive causal networks of three phases during 6 min post-stimulus resting epoch following acupuncture at GB40. It was clear that a bidirectional connection with maximal strength in the auditory network between the STG and AI appeared in all maps, moreover, increased causal influences emerged between the auditory network and others following acupuncture at GB40. Following acupuncture at KI3, several

causal outflows or inflows emerged between the SPL and motor network, auditory network and DMN in the second phase (Fig. 2e). The DLPFC began to have inflows from the postcentral gyrus, AI and STG at the last stage (Fig. 2f). In other words, increased both the memory and executive network connectivity with DMN, auditory network and motor network emerged, in comparison with the map of the first 2 min stage (Fig. 2d).
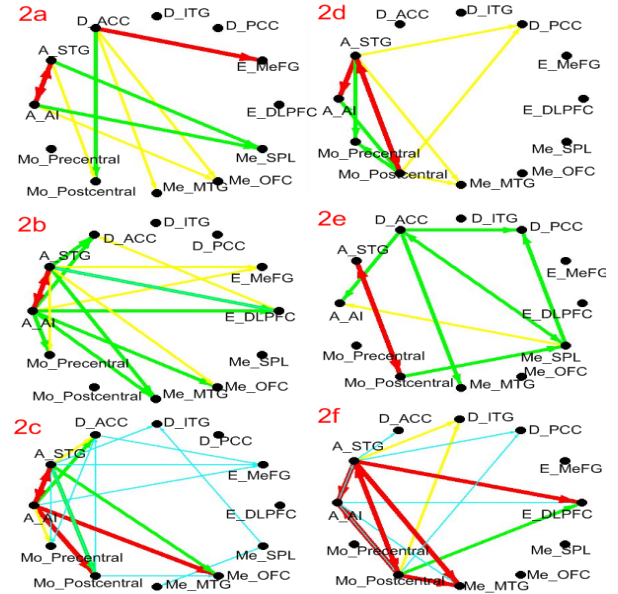

Fig. 2. mGCA results with significant connections (p < 0.05) for GB40 (2a, 2b and 2c) and for KI3 (2d, 2e and 2f). The thickness of line and divided into four grades with different colors (cyan-25%, yellow-50%, green-75%, red-100%) represented the relative strength of causal connections, while the arrows showed the direction for each pair of nodes. A_, D_, E_, Me_ and Mo_ represent auditory, default mode, executive, memory and motor networks.

IV. DISCUSSION AND CONCLUSION

In this study, we found that different evolutive causal influences within and across the RSNs can be modulated by acupuncture at GB40, comparing with acupuncture at KI3 as a control condition (belonging to the same nerve segment but different meridians). Our results provided additional evidence to support that acupuncture can exert sustained modulatory effects on the post-stimulus resting brain [9], [10]. In addition, the relatively functional specificity of acupoints can evolve as the function of time by comparing the effective connectivity patterns of brain networks. Following acupuncture at GB40, the STG and AI within auditory network appeared persistent bidirectional connection with maximal strength, and the interactions between the auditory network and others became more complex as time went on. For KI3, the causal connections within auditory network had lower strength and no dynamic consistency throughout the three phases.

The consistent brain networks detected by ICA involving DMN, memory network, executive network, auditory network and motor network were agreed with previous findings [11]. The GB40 is an audition-related acupoint from

a previous study [20]. Therefore, a bidirectional connection with maximal strength in the auditory network between the STG and AI emerged throughout three phases of 6 min post-stimulus resting epoch following acupuncture at GB40. As time went on, the STG and AI act as hubs converging both outflows and inflows of multiple neural pathways. The enhanced interactions also observed between the auditory network and others. Following acupuncture at KI3, the persistent bidirectional causal connection in auditory network didn't appear throughout three stages. There's a causal connection with maximal strength from the STG to AI during the first 2 min phase (Fig. 2d). In the second stage, no causal connection was found between the STG and AI (Fig. 2e). In the last phase, a strong connection from the STG to AI was observed and a weak connection emerged in the opposite direction (Fig. 2f). The results above tended to indicate that acupoint KI3 is irrespective of auditory function.

We found that increased both the memory and executive network causal influences with other networks as time passed following acupuncture at KI3, which was in accord with the investigation that acupuncture at KI3 could improve mood and cognitive functions of patients with Alzheimer's Disease [21]. During the first 2 min stage, there're only two inflows with medium strength (50%) coming into the MTG within the memory network, but no outflow or inflow from any nuclei in the executive network (Fig. 2d). There's still no causal connection within the executive network in the second phase, but the SPL within the memory network emerged five causal outflows and inflows from other networks (Fig. 2e). The SPL plays an important role in visual attention from a previous study [22]. During the last 2 min phase, the DLPFC had inflows from the postcentral gyrus, AI and STG. The DLPFC is located in the frontal lobe and associated with cognitive executive function [23]. Additionally, the PCC, as one of cognitive-related vital nuclei [24], always had two causal inflows incoming into it throughout the three phases following acupuncture at KI3, but none causal connection from it was found in the maps of three stages following acupuncture at GB40. The maps during the last 2 min stage both evolved to be complicated, and the causal connections following acupuncture at KI3 (Fig. 2f) had stronger strength than that following acupuncture at GB40 (Fig. 2c). These results may provide additional evidence in support of the relatively functional specificity of different acupoints.

In conclusion, the current study demonstrated that acupuncture at different acupoints could exert different causal influences within and across the RSNs and these effects can evolve as the function of time. Due to the sustained effects of acupuncture, the relatively functional specificity of acupoints may be unveiled as time passed. Our preliminary investigations may help to understand the neurophysiological mechanisms underlying acupuncture specificity.

REFERENCES

[1] Beijing, Shanghai and Nanjing College of Traditional Chinese Medicine. Acupuncture Institute of the Academy of Traditional Chinese Medicine. Essentials of Chinese acupuncture, Beijing, People's Republic of China: Foreign Language Press, 1980.

[2] NIH, "NIH consensus conference statement acupuncture," *JAMA,* vol. 280, pp. 1518-1524, 1998.

[3] K. Hui, *et al.*, "Acupuncture modulates the limbic system and subcortical gray structures of the human brain: evidence from fMRI studies in normal subjects," *Hum Brain Mapp,* vol. 9, pp. 13-25, 2000.

[4] J. Fang, *et al.*, "The salient characteristics of the central effects of acupuncture needling: Limbic-paralimbic-neocortical network modulation," *Hum brain mapp,* vol. 30, pp. 1196-1206, 2009.

[5] L. Bai, *et al.,* "Spatiotemporal modulation of central neural pathway underlying acupuncture action: a systematic review," *Current Medical Imaging Reviews,* vol. 5, pp. 167-173, 2009.

[6] D. Price, A. Rafii, L. Watkins, and B. Buckingham, "A psychophysical analysis of acupuncture analgesia," *Pain,* vol. 19, pp. 27-42, 1984.

[7] L. Bai, *et al.*, "Time-varied characteristics of acupuncture effects in fMRI studies," *Hum Brain Mapp,* vol. 30, pp. 3445-3460, 2009.

[8] L. Bai, *et al.*, "Acupuncture modulates temporal neural responses in wide brain networks: evidence from fMRI study," *Mol Pain,* 2010.

[9] R. Dhond, C. Yeh, K. Park, N. Kettner, and V. Napadow, "Acupuncture modulates resting state connectivity in default and sensorimotor brain networks," *Pain,* vol. 136, pp. 407-418, 2008.

[10] L. Bai, *et al.*, "Acupuncture modulates spontaneous activities in the anticorrelated resting brain networks," *Brain Res,* vol. 1279, pp. 37-49, 2009.

[11] J. Damoiseaux, *et al.*, "Consistent resting-state networks across healthy subjects," *Proc Natl Acad Sci USA,* vol. 103, pp. 13848-53, 2006.

[12] O. Demirci, *et al.*, "Investigation of relationships between fMRI brain networks in the spectral domain using ICA and Granger causality reveals distinct differences between schizophrenia patients and healthy controls," *Neuroimage,* vol. 46, pp. 419-431, 2009.

[13] C. Granger, "Investigating causal relations by econometric models and cross-spectral methods," *Econometrica,* pp. 424-438, 1969.

[14] W. Liao, *et al.*, "Small-world directed networks in the human brain: multivariate Granger causality analysis of resting-state fMRI," *Neuroimage,* vol. 54, pp. 2683-94, 2011.

[15] G. Deshpande, S. LaConte, G. James, S. Peltier, and X. Hu, "Multivariate Granger causality analysis of fMRI data," *Hum Brain Mapp,* vol. 30, pp. 1361-1373, 2009.

[16] M. Greicius, B. Krasnow, A. Reiss, and V. Menon, "Functional connectivity in the resting brain: a network analysis of the default mode hypothesis," *Proc Natl Acad Sci USA,* vol. 100, pp. 253-258, 2003.

[17] Q. Jiao, *et al.*, "Granger causal influence predicts BOLD activity levels in the default mode network," *Hum Brain Mapp,* 2010, DOI: 10.1002/hbm.21065.

[18] Y. Li, T. Adali, and V. Calhoun, "Sample dependence correction for order selection in fMRI analysis," *in Proc. ISBI, 2006,* pp. 1072-1075.

[19] M. Kamiński, M. Ding, W. Truccolo, and S. Bressler, "Evaluating causal relations in neural systems: Granger causality, directed transfer function and statistical assessment of significance," *Biol Cybern,* vol. 85, pp. 145-157, 2001.

[20] H. MacPherson, L. Thorpe, K. Thomas, and M. Campbell, "Acupuncture for low back pain: traditional diagnosis and treatment of 148 patients in a clinical trial," *Complement Ther Med,* vol. 12, pp. 38-44, 2004.

[21] M. Lee, B. Shin, and E. Ernst, "Acupuncture for Alzheimer's disease: a systematic review," *Int J Clin Pract,* vol. 63, pp. 874-879, 2009.

[22] J. C. Culham and N. G. Kanwisher, "Neuroimaging of cognitive functions in human parietal cortex," *Current Opinion in Neurobiology,* vol. 11, pp. 157-163, 2001.

[23] B. Elsa, A. Philip, P. Kevin, and J. Rosalie, "On age differences in prefrontal function: The importance of emotional/previous cognitive integration," *Neuropsychologia,* vol. 48, pp. 319-333, 2010.

[24] D. Sridharan, D. Levitin, and V. Menon, "A critical role for the right fronto-insular cortex in switching between central-executive and default-mode networks," *Proc Natl Acad Sci USA,* vol. 105, pp. 12569-74, 2008.